Photophysics of buckminsterfullerene and other carbon cluster ions

S. C. O'Brien,[a] J. R. Heath,[a] R. F. Curl, and R. E. Smalley
Rice Quantum Institute and Department of Chemistry, Rice University, Houston, Texas 77251

(Received 13 May 1987; accepted 7 October 1987)

The laser-induced fragmentation behavior of positive carbon cluster ions has been investigated by tandem time-of-flight techniques for the jet-cooled clusters up to 80 atoms in size. Two distinct photophysical regimes were found. The first applies to clusters with 34 atoms or more, all of which dissociate to produce even numbered fragments. Large even clusters fragment by the loss of the high energy species C_2, odd ones lose a C atom. The second regime applies to clusters composed of 31 or less atoms, all of which fragment by the loss of C_3. These two regimes are sharply separated by C_{32}^+ which fragments to produce small cluster ions in the 10–19 atom size range. Fragmentation of the large clusters occurs on a microsecond or faster time scale only at very high levels of excitation (> 12.8 eV). These photophysical results are interpreted as consequences of the large even clusters having edgeless, spheroidal cage structures while the small ones have linear chain or ring structures.

I. INTRODUCTION

As a result of the recent flurry of experimental[1–13] and theoretical[14–26] work on carbon clusters, there is great interest in obtaining detailed knowledge of the structures these clusters assume. In particular, it is clear that the 60th cluster of carbon is something quite special. The fact that C_{60} can be made to dominate the carbon cluster distribution led to the suggestion that it may have the shape of a truncated icosahedron. Analogy to the geodesic architectural inventions of Buckminsterfuller prompted the name "buckminsterfullerene" for this remarkable structure.[4]

While the experimental results and arguments for this closed carbon shell model of C_{60} are compelling, they are indirect and rather involved. Unambiguous structural determination remains elusive, although recent spectroscopic investigations have shown C_{60} to have a very special electronic structure.[27,28] In the interim, therefore, we have turned to the question of the photophysics of these clusters as an independent probe of the cluster structure, stability, and bonding.

As detailed below the carbon cluster system does have a highly colorful and striking photophyics that shows quite clearly that there are at least two distinct types of clusters. The photophysics of large carbon clusters, including buckminsterfullerene, is fully consistent with the model of even clusters having closed spheroidal shell strucutures.[5(a)]

II. EXPERIMENTAL

Photofragmentation experiments were conducted on the positive ions of carbon clusters. The apparatus and cluster source was similar to that discussed in previous work,[6,7,29,30] but in contrast with the scheme used in previous publications, the cluster target was located external to the main vacuum chamber. This allowed much easier access to the target and a much longer nozzle-to-skimmer spacing (70 cm) permitting the use of directional nozzles with a 15° internal angle cone to increase both cooling and on axis jet intensity. Helium densities of 0.2 atm above the target combined with the nozzle flow geometry give an estimated 3×10^4 collisions per C_{60}^+ ion during the expansion.

The cold positive ions were generated by the vaporization of a graphite target inside the nozzle which produces the supersonic jet.[6,9,31,32] Since no ionization laser was needed, the possibility of fragmentation or ionization cross section artifacts on the cluster intensity profile was eliminated, and the internal temperature of the clusters should be low. Under the clustering conditions used in most of the experiments reported here, the positive cluster ion profile was measured to be peaked around C_{100}^+ with a strong C_{60}^+ peak relative to its neighbor clusters ($\times10$) with almost nothing smaller than about 40 atoms, and no odd clusters.

For certain experiments the small clusters were the species to be investigated and the vaporization laser was fired well before the maximum of the He carrier gas arrival above the target. Under these conditions the average cluster profile peaked around C_{40}^+ with odd clusters smaller than C_{38}^+ having similar intensities to the even ones. These conditions were very unstable and the cluster profile showed large fluctuations.

In the tandem time-of-flight mass spectrometer (Fig. 1) ions were pulse extracted with 2000 eV from the molecular beam and entered a 3 m flight tube. The molecular beam velocity was removed by a static deflection field and the ion beam was focused by two einzel lenses. The ions then entered a vacuum chamber detailed in Fig. 2 where the photophysical experiments were performed.

The mass selection was accomplished by a two-stage grid assembly placed perpendicular to the ion beam. The outer two plates were grounded and the center plate was held at a potential higher than the energy of the ions, thus all ions were reflected by the first stage. At the time that the desired cluster packet arrived, the center grid was pulsed to ground allowing the ions to traverse the first region. The grid was then pulsed back to its original voltage reflecting later arriving ions. In three of the data sets (Fig. 4) this mass gate was improperly operated such that about 20% of the total cluster signal was for an adjacent cluster; however, all other mass

[a] Robert A. Welch Foundation Predoctoral Fellow.

 0021-9606/88/010220-11$02.10

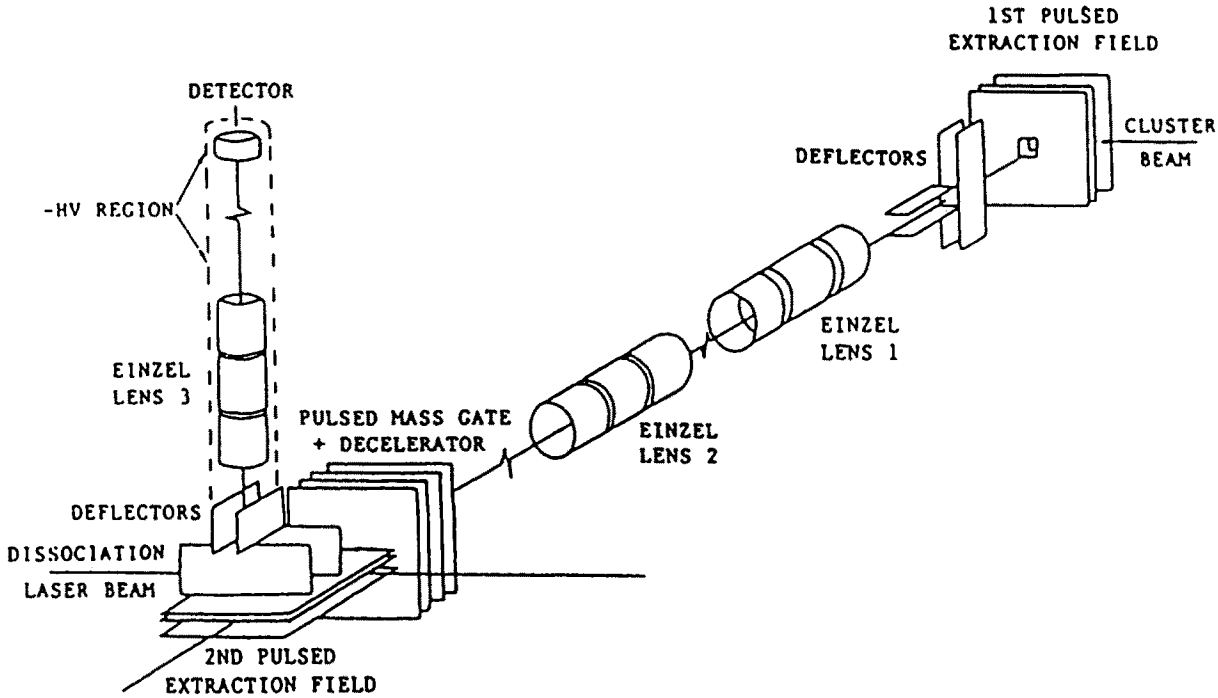

FIG. 1. Overview of tandem time-of-flight mass spectrometer. The molecular beam enters the extraction region of the primary mass spectrometer. 2000 V is pulsed across the extraction grids, the molecular beam velocity is removed by one set of deflectors, and the beam is spatially focused by two einzel lenses. The ions then enter another vacuum chamber (detailed in Fig. 2) where the fragmentation experiments are performed.

spectra have the parent ion isolated from the others with a ratio of greater than 500:1.

The ions were decelerated in the region after the mass selection to facilitate excitation and extraction. After leaving this region the ion energy was about 20% of the initial energy (400 eV). After deceleration, the ions entered a region where they were irradiated by the dissociation laser. The lasers used were either the second, third, and fourth harmonics of a DCR-2 Nd:YAG laser or a Lumonics excimer laser operating on ArF (193 nm) or KrF (249 nm) with unstable resonator optics. There was no difference in dissociation patterns observed for any wavelength, and consequently the laser was chosen for either photon energy or maximum fluence. After laser excitation, the clusters continued to drift for several cm into the extraction region of the first stage of the perpendicular mass spectrometer.

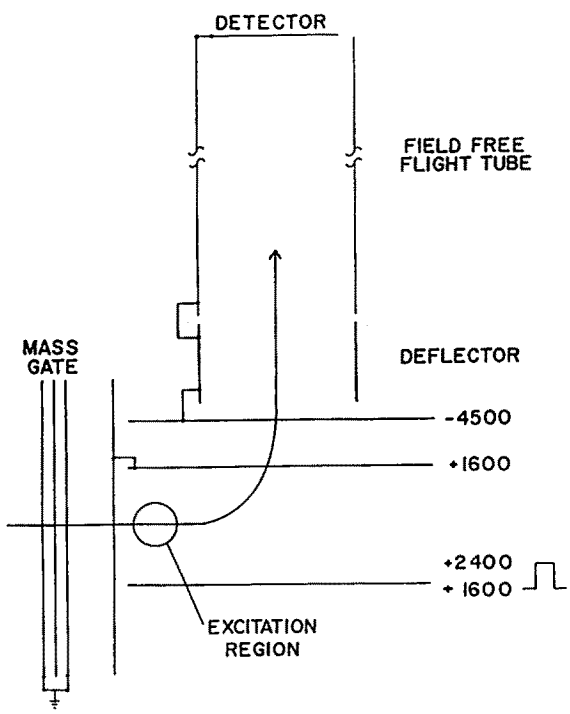

FIG. 2. Detailed diagram of ion chamber optics and geometry showing mass gate, excitation region, extraction optics, and field free flight tube.

The laser excitation region was separated from the center axis of the second mass spectrometer to compensate for the radius of curvature of the ions as they were pulsed into the flight tube. The extraction pulse was varied in time to allow the ions to exit the extraction stack due to heavy ions having a larger turning radius than light ones. The first stage of the mass spectrometer was floated at the deceleration voltage to allow field free flight from the laser interrogation region to the extraction region. The first stage stack was pulsed with 800 V to extract the ions. The second region voltage was about 6100 V with the exact voltages set for a well focused ion packet at the detector according the standard TOF-MS procedures.[33] The flight tube was 1 m long and floated along its length at the final extraction potential for field free flight throughout the tube. The perpendicular ion beam velocity was removed by a static deflection field and the ions are collimated inside the flight tube by another einzel assembly. The detector was a pair of microchannel plates with the front plate biased at the flight tube potential. The signal was capacitively coupled into a preamplifier and this produced a ringing to the higher time (mass) side of the parent ion peaks. On several data sets this appeared to be signal from higher mass ions but it was only an artifact.

Two types of fragmentation experiments were performed. In the first, after mass selection the clusters were dissociated by a laser pulse, and the fragments were observed in the second perpendicular mass spectrometer. In the second type of experiment, metastable clusters were produced before the initial extraction, and were then mass selected and analyzed in the tandem mass spectrometer. The amount of time the clusters were allowed to fragment before the final analysis was the difference between the two experiments: 3 μs in the first vs 120 μs in the second.

The dependence of the daughter ions upon laser fluence was obtained either by measuring the fragment intensity while varying the laser fluence under conditions of constant spatial profile or simply by observing the mass spectrum changes with laser power. Artifacts having to do with poor overlap and inhomogeneous laser beam profiles generally reduce the apparent order of the curve of signal vs laser fluence but do not increase it (if the laser spatial profile was constant), thus any curvature observed in such a plot must have resulted from a multiphoton process.

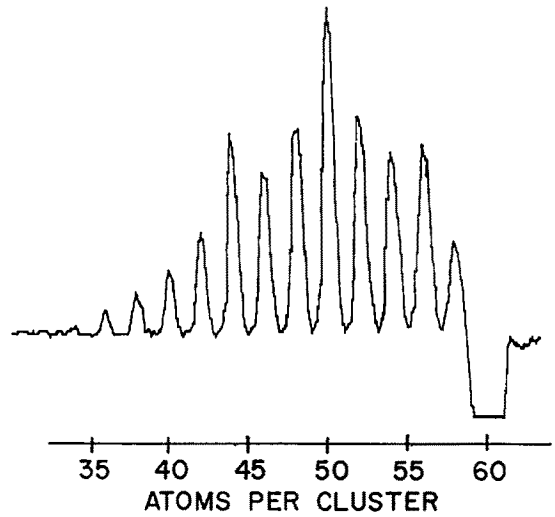

FIG. 3. C_{60}^+ mass selected and fragmented with 15 mJ cm^{-2} ArF (193 nm) excimer light. Two data sets were taken on alternating experimental cycles with the laser on and off. The two sets were then subtracted resulting in the depletion of parent ions and enhancement of daughters. C_{50} is a slightly preferred daughter ion.

III. RESULTS

A. Fragmentation paths of the small clusters ($n<32$)

Geusic *et al.*[3] have shown that the fragmentation of all carbon clusters with 20 or less atoms proceeds by the same primary dissociation channel: loss of C_3. We have reproduced their results and extended them to larger clusters. Fragmentation by successive loss of C_3 units was found to apply to all clusters up to C_{32}^+. As will be clear later, this 32nd cluster serves as an amazingly sharp dividing line in the carbon cluster photophysics.

B. Fragmentation paths of the large clusters ($n>32$)

In contrast to the C_3 loss of the small clusters, all even numbered clusters with $n > 32$ were found to fragment by the loss of C_2. This is shown in the particular case of C_{60}^+ in Fig. 3, where a 15 mJ cm^{-2} pulse of 193 nm light has produced not only C_{58}^+, but also even numbered fragments down into the 30 atom range. At lower fluences, C_{58}^+ is the dominant fragment. The smaller fragments grow in sequentially as the laser fluence is increased. The C_{60}^+ cluster therefore appears to fragment either by successive C_2 losses:

$$C_{60}^+ + nh\nu \rightarrow C_{60}^{+*} \rightarrow C_{58}^{+*} \rightarrow C_{56}^{+*} \rightarrow C_{54}^{+*} \cdots$$

or by single step elimination of even units:

$$C_{60}^+ + nh\nu \rightarrow C_{60}^{+*} \rightarrow C_{60-e}^+ + C_e,$$

i.e.,

$$\begin{aligned} C_{60}^+ + nh\nu \rightarrow C_{60}^{+*} &\rightarrow C_{58}^+ + C_2 \\ &\rightarrow C_{56}^+ + C_4 \\ &\rightarrow C_{54}^+ + C_6 \\ &\rightarrow \cdots \end{aligned}$$

Neither the fragmentation patterns nor the fluence dependencies can distinguish between these two mechanisms, but it must be kept in mind that C_2 is a relatively high energy species, and the repeated sequential process will remove a great deal of energy. We shall see that the explanation of some experiments demands the single step loss of a neutral fragment with four, six, eight, or an even larger even number of carbon atoms. In any event, an excited carbon cluster fragments by ejecting a neutral cluster (C_e) containing a small even number of carbon atoms. The large fragment ion produced may still have enough internal energy to fragment again. This will be discussed in detail later in the paper.

As different choices are made of the large even cluster to be mass selected and studied, we found that not only C_{60}, but all even numbered clusters larger than 32 fragmented by the loss of C_e. For example, Fig. 4 shows the photofragmentation pattern for clusters in the range of 80, 74, and 68 atoms, respectively. All of these large even clusters fragment by the same C_e loss process. Note that the daughter fragments at C_{70}^+, C_{60}^+, and C_{50}^+ are a bit more favored than the others. Furthermore, note that C_{60}^+ (for example) appears in higher contrast to its neighboring clusters when it is a high order daughter from C_{80}^+ than it appears when made as a low order daughter from C_{68}^+.

When one of the large odd numbered cluster ions is examined in this photolysis apparatus, a very similar fragmentation pattern is seen. As shown in Fig. 5 for the case of C_{59}^+, such an odd cluster fragments to produce even numbered cluster ions with the same distribution as if C_{60}^+ had been the parent ion. In particular, notice in this figure that there is a slight but definite local preference for the C_{50}^+ cluster. This is about the same preference as that seen in Fig. 3 where the fragments did come from C_{60}^+.

C. The dividing cluster: C_{32}

While Figs. 3–5 seem to suggest that higher laser fluences would only produce further C_e loss, this is not the case. As shown in Fig. 6, increasing the laser fluence ultimately reveals a very dramatic and abrupt end to the loss process at C_{32}^+. Although a very small amount of C_{30}^+ is

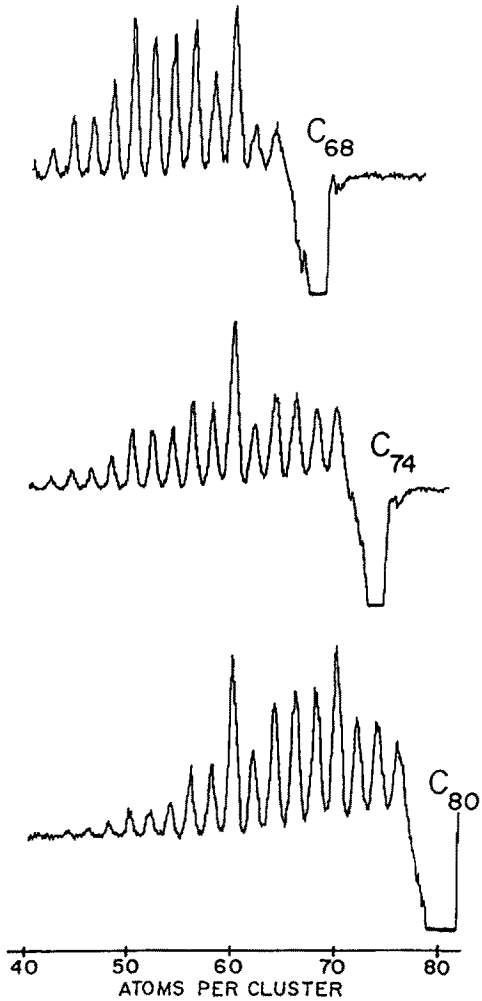

FIG. 4. ArF (15 mJ cm^{-2}) fragmented large even carbon clusters. The top is C_{68}^+ with a small amount of C_{66}^+ (10%). The middle is C_{74}^+ with a little C_{72}^+ (10%). The bottom is C_{80}^+ with about 20% C_{78}^+ and 10% C_{82}^+. There is no difference in the fragmentation behavior amongst the large even clusters, the primary photophysical process is the loss of two atoms with C_{50}, C_{60}, and C_{70} favored daughters.

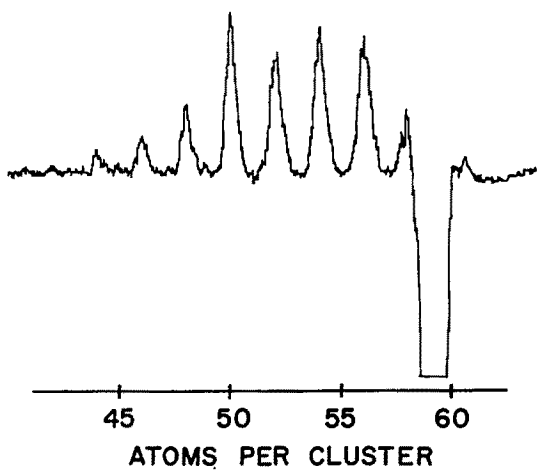

FIG. 5. Mass spectra of C_{59}^+ fragmented by 25 mJ cm^{-2} at 266 nm. The fragments are even cluster ions of size 58,56,... with C_{50}^+ a favored product similar to Fig. 3.

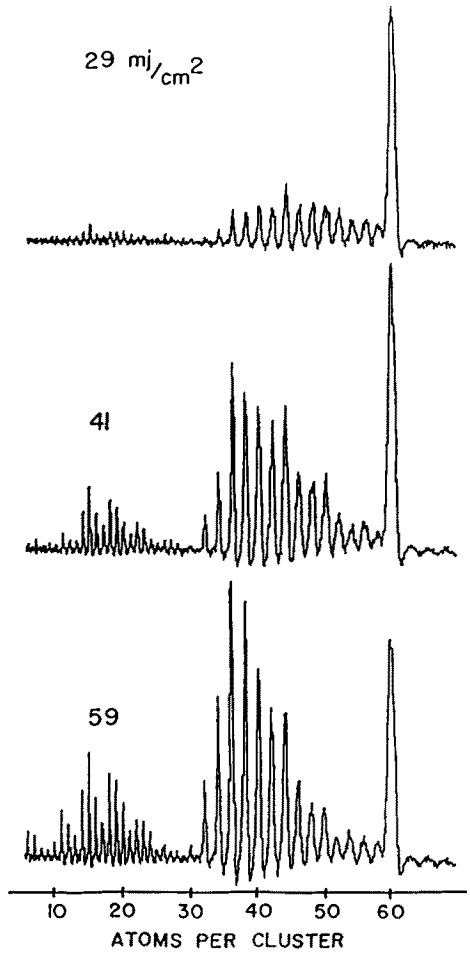

FIG. 6. Mass spectra of C_{60}^+ fragments obtained with variable amounts of 353 nm light. The fluences (in mJ cm^{-2}) are 29 for the top, 41 for the middle, and 59 for the bottom. The detection of fragments is optimized near 30 atoms. The slower growth of the smaller fragments indicates that they require more excitation to form than the larger ones. The drastic change in the fragment pattern at 32 indicates this is the last stable cage structure.

sometimes seen, most experiments we have tried in this fluence range showed a very abrupt termination at the 32nd cluster. Figure 7 is a particularly vivid demonstration of this effect. After C_{32} there is a gap in fragment cluster ions observed down to about C_{25}^+. Figure 6 also illustrates the higher photon order of the small fragments vs the larger ones, the distribution of fragments peaks at lower and lower masses as the laser fluence increases.

Figure 8 shows that this same photophysics applies to cluster ions in the size range 30–34. The top trace here shows that C_{30}^+ fragments by the loss of C_3. The bottom trace shows C_{34}^+ fragmenting primarily by loss of C_2. But C_{32}^+ in the center trace clearly does neither. Instead its positively charged fragments are concentrated in the 10–19 atom size range. This extensive fragmentation was found at the lowest usable laser fluences.

D. Valence isomers of the carbon cluster ions

It is not only possible but likely that many of these carbon clusters will initially exist in more than one valence isomer. Although these other isomers are interesting in themselves, the primary intent of this work is to determine the photophysical behavior of the most stable possible form of each cluster ion. In the case of the large even clusters such as

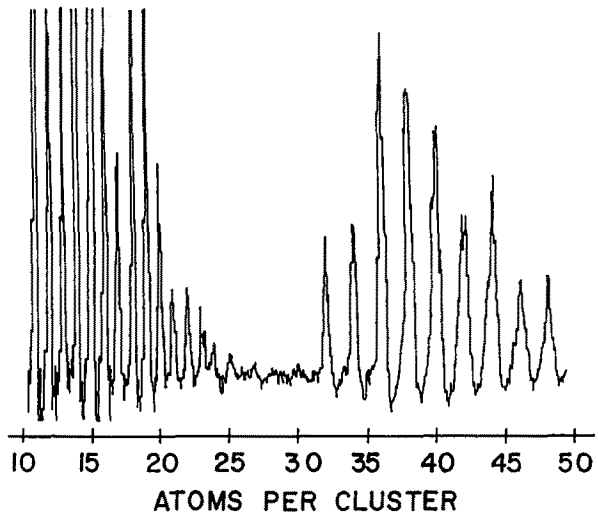

FIG. 7. Enlarged region of fragments from C_{60}^+ near 32 made with 55 mJ cm^{-2} at 353 nm. The large ratio of 32 to 30 or 29 shows that 32 does not lose 2 or 3 atoms.

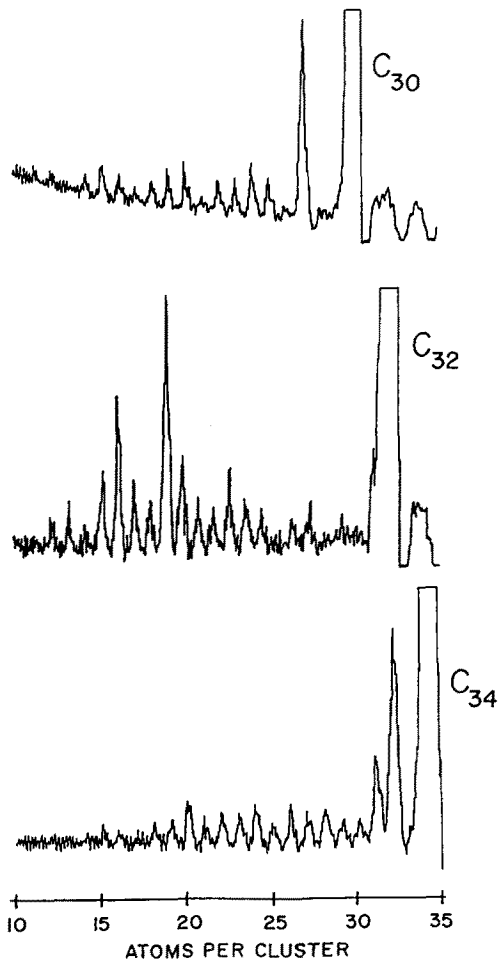

FIG. 8. Photofragmentation done with high fourth harmonic fluence (25 mJ cm^{-2}) on C_{30}, C_{32}, and C_{34} ions showing the change in fragmentation pattern between large and small even clusters. C_{30}^+ always loses three atoms; however, the dissociation of the next few even clusters is critically dependent on clustering conditions. C_{32}^+ usually loses a large number of atoms but can lose C_3. C_{34}^+ usually loses two atoms but can lose three as shown. The signal to higher mass of the parent ions is due to inductive ringing of the detection circuit.

C_{60}, the most stable form is taken to be that which survives the most intense clustering conditions in the nozzle, i.e., when the vaporization laser is fired near the center of the helium pulse. With this timing, the carbon plasma is rapidly thermalized, diffusional loss to the nozzle walls is minimized, and the maximum possible number of reactive collisions will take place between the various carbon species. For the large even clusters the less stable (more reactive) valence isomers should then be removed from the cluster beam simply by running at these extreme nozzle conditions.

However, in order to study the more reactive clusters such as the large odd numbered species or those in the C_{25}–C_{40} range, it is necessary to operate the nozzle with milder conditions by firing the vaporization laser early in the helium pulse where there are fewer collisions between the clusters, and consequently less opportunity for alternative valence isomers of the clusters to react. Unfortunately, these operating conditions are somewhat unstable in that the nature of the clusters produced appears to vary unreproducibly. This was particularly clear in experiments of the sort shown in Fig. 8. The C_{32}^+ cluster here shows negligible intensity in the nearby daughter channels, but the same cluster prepared under roughly the same nozzle conditions at a different time was found to have a small proportion which did fragment by the loss of C_3. This change in fragmentation pattern suggests the existence of another isomer of C_{32}^+. In the C_{34}^+ fragmentation picture at bottom of Fig. 8, the C_{31}^+ daughter signal is thought to arise from a less favored valence isomer, the C_{32}^+ daughter arising from the more stable isomer. The relative intensity of these two signals appear to be sensitively dependent upon the clustering conditions.

Figure 9 provides further evidence of multiple valence isomers in the cluster beam. Here C_{36}^+ is seen to fragment extensively at only 1 mJ cm^{-2} to produce daughters in the 18–22 size range. Only at much higher fluences does C_{34}^+ appear as a daughter ion. We interpret this as good evidence for the presence of two distinct C_{34}^+ species in the cluster beam: (1) a strongly absorbing, but poorly formed cluster which fragments extensively at low fluence, and (2) a much more tightly bound species which absorbs weakly and fragments only at high laser fluences in a primary process which involves C_2 loss. Upon varying the nozzle timing, the type (2) cluster was found to be strongly favored when the vaporization laser fired nearer the center of the helium pulse. We interpret this as indicating that the type (2) cluster is much more stable.

Even in the case of C_{60}^+ there is evidence for other valence isomers in the supersonic beam when the vaporization laser is fired sufficiently early in the helium pulse. Figure 10 shows one such example. Here with low fluence 3.6 eV laser radiation, there is a wide distribution of fragments. In particular, a substantial ion signal much larger than seen at low fluence in Fig. 6 is observed in the region of 10–30 atoms. The independence of this low mass ion signal on the laser fluence indicates that production of these small fragments has saturated.

The valence isomer responsible for this low fluence fragmentation, let us label it C_{60i}^+, can be readily removed by operating under more intense clustering conditions. Since it

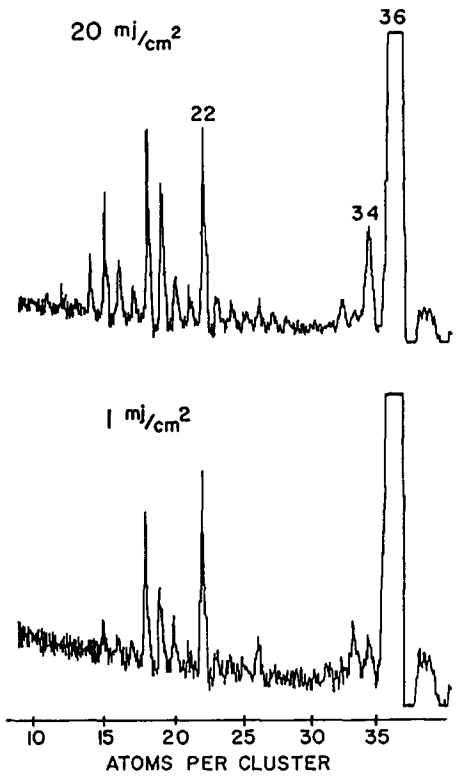

FIG. 9. Mass spectra of the fragments of C_{36}^+ at two fluences of 266 nm light. The products present at 1 mJ are probably from a different isomer than the 34 atom daughter in the 20 mJ picture.

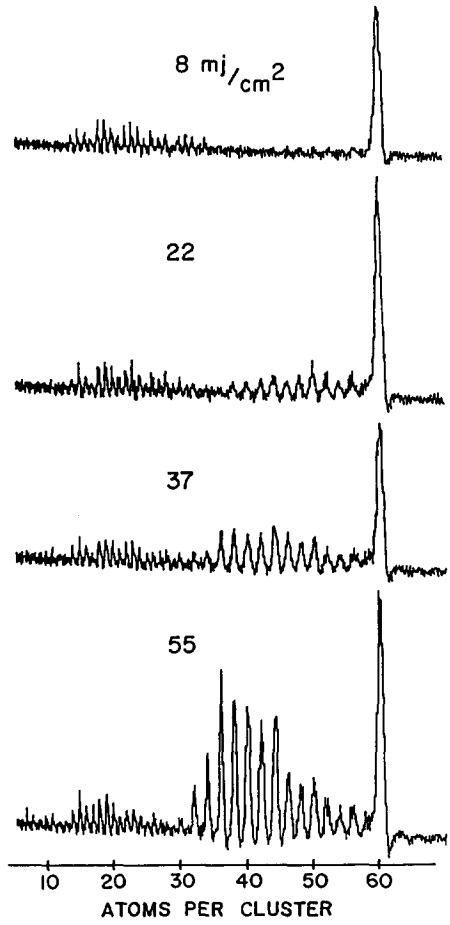

FIG. 10. C_{60}^+ fragmentation mass spectra optimized near 15 atoms for increasing fluences (mJ cm^{-2}) of 353 nm light. The top is at 8, second at 22, third at 37, and bottom at 55. All size fragments appear at 8 mJ in equal amounts. The saturation of the small fragments plus their appearance for small fluence indicates that they are primary fragments and not multiphoton granddaughters. This is evidence for a second isomer of C_{60}. Similar data resulted for all other large even clusters.

is so readily fragmented at mild laser fluence, one might expect that it could be removed from the molecular beam by laser photolysis. In fact such an experiment was successful. A 10 mJ cm^{-2} pulse from a KrF laser was found to be sufficient to eliminate these readily fragmented C_{60i}^+ clusters.

One can obtain a rough idea of the one-photon absorption properties of a cluster just by observing the extent of fragmentation at different laser wavelengths. Many structures for a cluster composed of 60 carbon atoms would be expected to be effectively black, having strong absorptions throughout the visible spectrum. In fact the unstable valence isomer C_{60i}^+ did behave in this way. It was easily fragmented with low fluences of all harmonics of the Nd:YAG laser, including the green second harmonic. The stable, dominant C_{60}^+ cluster, on the other hand, required over 60 mJ cm^{-2} irradiation at 532 nm before any fragmentation could be seen at all. The initial indication is, therefore, that C_{60}^+ is nearly transparent in the visible. Recent spectral experiments with C_{60} van der Waals clusters[27] have shown similarly weak absorption in the visible for neutral C_{60}—strong evidence that it is a cluster without dangling bonds or long unsaturated chains.

E. The fluence dependence of C_{60} fragmentation

We have measured the intensity of the various photofragment daughter ions as a function of laser fluence for a variety of excitation lasers. Figure 11(a), e.g., shows the low fluence dependence of the C_{58}^+ daughter ion produced by photolysis of C_{60}^+ with a KrF laser at 4.9 eV. A rough fit to the C_{58}^+ curve show this photoprocess requires three photons of the KrF laser. In Figs. 11(b) and 11(c) are shown the fluence dependence of the first two daughter ions taken simultaneously. Note that both curves show a substantial induction fluence and that C_{56}^+ is clearly formed in a higher order process than C_{58}^+. Similar results were obtained with the ArF laser at 6.4 eV. Although these measurements are difficult to make accurately, the effect of imperfections in the measurement in such experiments is generally to reduce the apparent order of any photofragmentation.[29] Our conclusion is that the first fragments of C_{60}^+ are detected only after absorption of at least three photons of ArF radiation (and possibly more).

As with most time-of-flight measurements of photofragmenting systems, the apparatus used in these studies can detect fragmentation only if it occurs prior to the acceleration of the ions down the flight tube. In our apparatus this critical time is roughly 3 μs. While for small clusters even mild excitation above the dissociation threshold will result in fragmentation on a submicrosecond time scale, these large carbon clusters are quite different. In the case of C_{60}^+, e.g.,

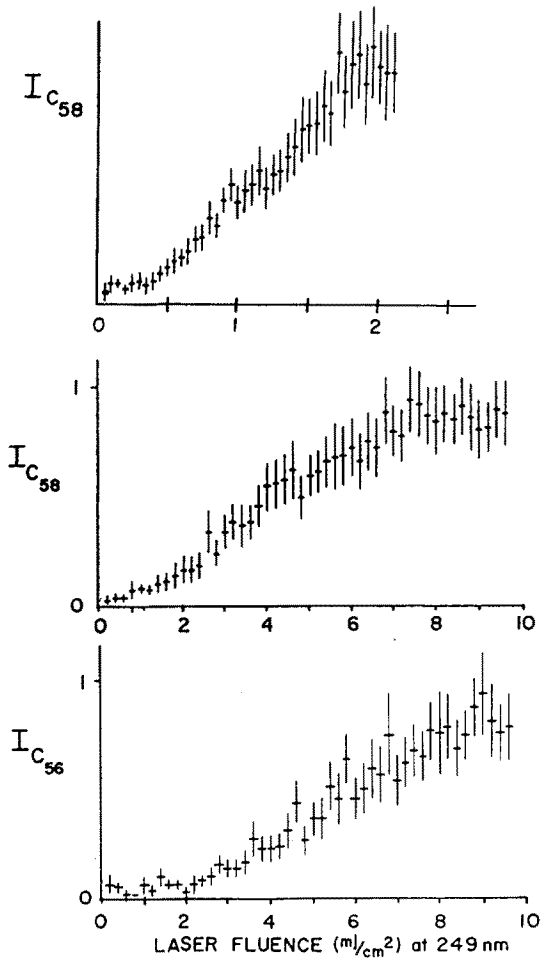

FIG. 11. KrF (249 nm) power dependence for C_{58} and C_{56} daughter ions of C_{60}^+ proving multiphoton dependence for C_{58} with higher order for C_{56}. The top data set was taken on the C_{58}^+ ion for a low fluence range while the bottom two data sets were taken simultaneously with identical y axes. No linear power scan was ever seen for ArF on C_{60}^+ or any other cluster between 50 and 70.

there are 174 vibrational modes. If the laser energy is randomly distributed among these modes, RRKM estimates of the dissociation rate for a process with a 3 eV activation barrier show that excitations of at least 20 eV will be required. Obviously the normal methods for photophysically bracketing the binding energy cannot work for large molecules.

F. Long time scale metastable decay

Although the data discussed thus far are sensitive only to fragmentations occurring within the first 3 μs after the laser pulse, there is a way of looking at much longer time scale dynamics. Referring back to the overall apparatus design sketched in Fig. 1, it is possible to direct the photolysis laser down the original supersonic cluster beam and hit the clusters long before the final analysis in the second flight tube. The laser is fired and after an initial evolution period (time 1) metastable clusters (clusters which have not yet dissociated) are accelerated out of the molecular beam, along with all other ions, down the first flight tube and "mass gated" before they arrive at the second extraction region. Any fragmentation occurring along the first flight tube while the clusters drift (for time 2) will not significantly affect their velocity. They will still be accepted by the mass gate and enter the second extraction region along with their parent ions even though their mass is now changed. The presence of these long time scale daughter ions is then revealed by the second time-of-flight mass analysis.

Figure 12 shows the result of long time fragmentation spectra obtained with four different choices of the mass-gated "parent" cluster ions. In all four cases, the initial delay to the first extraction (time 1) was 1 μs. All fragments observed in these mass spectra resulted from dissociations occurring in the subsequent flight during time 2, which was on the order of 120 μs. We can be sure that all fragments were laser induced, since none of the daughter ions were observed

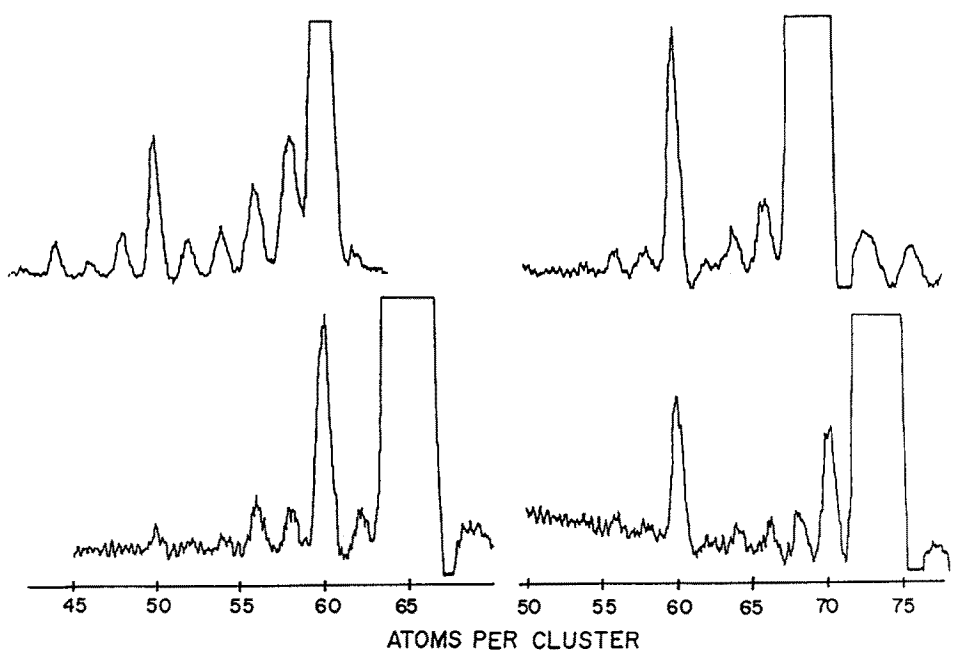

FIG. 12. Metastable TOF mass spectra for 60, 66, 70, and 74 atom clusters. The clusters were irradiated 1 μs before the first extraction pulse with 15 mJ cm^{-2} ArF. After the 120 μs travel in the first flight tube, they were mass gated and analyzed in the second mass spec. Daughter ions retain the parent velocity, thus they are transmitted by the mass gate. The largest intensity fragment is the C_{n-2} ion (about twice the other fragment heights). C_{60}^+ (and slightly C_{70}^+ and C_{50}^+) is a bottleneck in the unimolecular fragmentation path. This special nature of C_{60}^+ was less evident in the short time experiments of Fig. 4 because in order to show fragmentation on the short time scale the parent ion has higher internal energy and the fragmentation rate should vary much more slowly with binding energy.

without the initial fragmentation laser pulse fired down the supersonic beam.

The mass spectra in Fig. 12 have two things in common: (1) the C_{n-2}^+ fragment is the dominant daughter (off-scale) and (2) each displays a strongly preferred fragment, which is either C_{70}^+, C_{60}^+, or C_{50}^+, among the higher-order granddaughters. While some indication of this preference for C_{70}^+, C_{60}^+, and C_{50}^+ granddaughters was seen in the short time scale fragmentation results of Figs. 3, 4, and 5, there is clearly a far more pronounced preference for these special clusters in the long time results. This large fragmentation ratio only occurs when the clusters are allowed to evolve for long times after laser excitation before analysis.

A rough indication of the rate of fragmentation is seen in Fig. 13 which shows the C_{n-2}^+ daughter ion signal observed from C_{60}^+ and C_{74}^+ fragmenting in the first time of flight as a function of the time delay of excitation before extraction. The daughter ion signal can come only from metastable parents, thus, this is a plot of the unimolecular decay rate of metastable carbon cluster ions. These signals represent ions which had a mass during acceleration of 60 and 74 carbon atoms, respectively, and had sufficient energy to undergo unimolecular decay during the 120 μs flight down the first drift tube. Because of the possibility of fragmentation before and during the initial acceleration, the identity of the true parent ions is slightly ambiguous, but the difference in the lifetimes suggests a difference between the behavior of C_{60}^+ and C_{74}^+. Similar curves were obtained for all clusters studied in the range of 50–80 atoms with shorter lifetimes for clusters other than C_{60}^+. As seen in Fig. 13 the difference is not small; the daughter ion of C_{74}^+ decays to zero signal in 40 μs, but the C_{60}^+ product remains measurable even after 125 μs.

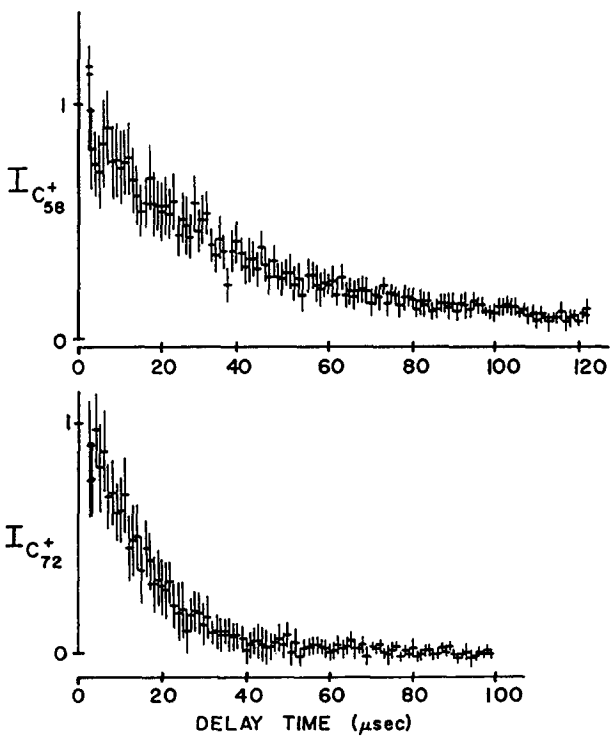

FIG. 13. Apparent lifetime for unimolecular decay of C_{60}^+ and C_{74}^+ excited with 15 mJ cm^{-2} at 193 nm a variable amount of time before the primary extraction pulse. The y axis is the intensity of the C_{n-2}^+ daughter with the x axis the delay between the excitation laser and the extraction pulse in μs. The curve represents the decay of the parent ion before the first mass spec. extraction. C_{60}^+ is more stable than C_{74}^+ as shown by the longer lifetime.

IV. DISCUSSION

Previous experiments from this group[4–7] have provided extensive evidence that C_{60} and the other large even numbered clusters are remarkably unreactive, this lack of reactivity being specially pronounced for C_{60}. As we have discussed in detail,[1,35,36] we believe there is only one consistent explanation which accounts for all known observations: the large even numbered clusters are closed cages consisting of 12 pentagons and $(n-20)/2$ hexagons. The special inertness of the 60th cluster then arises from symmetry. In the form of a truncated icosahedron, C_{60} achieves a perfectly even distribution of the strains, and a highly aromatic, closed shell electronic structure. Consideration of strain distribution and adjacency of pentagons then predicts that C_{70} should be the next most stable cluster,[5,20] in agreement with experiment.

As discussed below, the new photophysical results on the large clusters are amazingly consistent with this closed spheroidal cage model. This model was developed without consideration of carbon cluster photophysics and yet it fully explains the body of this work. In fact, we have been unable to find any other model for the structure of these clusters which is equally capable of predicting these observations. We begin discussion by summarizing these new experimental facts.

(1) Even numbered carbon cluster ions from 34 atoms to the highest studied (C_{80}) photofragment to produce only even numbered daughter ions (Figs. 3 and 4). The lowest order observed photoprocess is the loss of C_2. The odd clusters in this size range also fragment to produce only the even-numbered daughters (Fig. 5).

(2) There is an abrupt change in the fragmentation pattern when the parent ion is reduced in size. Below C_{32}^+ no fragments are seen of size $n-2$. Instead, all such smaller clusters fragment by the loss of C_3.

(3) Higher-order photoprocesses produce successively smaller even clusters until, at C_{32}^+, a gap appears in the high-order granddaughter distribution. Further fragments are seen primarily in the range of 7–25 atoms (Figs. 6 and 7). Fluence dependence studies (Fig. 11) suggest that the fragmentation involves more photons as more atoms are lost.

(4) Daughter ions with 50, 60, and 70 atoms are somewhat prominent for short time scale (4 μs) fragmentation (Fig. 4), but are markedly more prominent for long time scale fragmentation (Fig. 12).

(5) Less stable, more reactive valence isomers of the large carbon clusters can be produced in the beam. Fragmentation patterns are found which depend strongly upon nozzle conditions for C_{32}^+ and C_{34}^+. All large clusters, including C_{36}^+ (Fig. 9) and C_{60}^+ (Fig. 10), can be made to exhibit non-standard fragmentation patterns at low fluence when the vaporization laser is fired early in the helium pulse.

As originally observed by Rohlfing, Cox, and Kaldor,[2] there is a remarkably distinct gap in the observed carbon cluster distribution between about 28 and 40 atoms when these clusters are prepared in a supersonic laser–vaporization source. The lower group exhibits both even and odd clusters and lose C_3 upon photolysis, the higher group consists primarily of only even clusters which we now find lose C_2 when they fragment. These two abundance patterns together with their associated distinct photophysics strongly suggests that there are two distinct types of structures involved. Both theory[14,15,37] and experiment[7,34] agree that the small clusters are largely one or two dimensional: linear chains for the smaller ones and monocyclic rings for the larger. As Geusic *et al.* demonstrated[3] the smaller of these species fragment by the loss of C_3, and the new results above show this behavior continues up to the 31st cluster. Fragmentation by loss of C_3 in these clusters may result from C_3 being the most stable possible small fragment, and the lack of any strong preference for one particular large cluster fragment over another.

In comparison with C_3 and the higher clusters of carbon, C_2 is quite a weakly bound, high energy species.[37] It is, therefore, quite remarkable to find C_2 suddenly becoming the preferred fragment as the cluster size increases. The ejection of this high energy neutral implies that (1) the $n-2$ ion fragment must be particularly stable, (2) this stability must be sensed at the transition state in the fragmentation process, and (3) the corresponding transition state for C_3 loss must lie at considerably higher energy. In the spheroidal shell model it is fairly easy to see how such a combination of circumstances could come about. For such shells, only the even numbered clusters can close. Shells containing an odd number of atoms are possible, but all such structures must have several dangling bonds. This nicely explains why the even clusters would be so much more stable.

A. A concerted C_2 loss mechanism

Figure 14(a) shows how a C_n spheroidal shell with a fused five-membered ring system could lose C_2 and rearrange into a C_{n-2} spheroidal shell. The resulting structure has two pentagons and one less hexagon as required to maintain the closed spheroid. The four-center transition state involved in this process is forbidden in the Woodward–Hoffman sense, and such a concerted C_2 loss mechanism would ordinarily not be expected to be important. Nevertheless, it may be the lowest available fragmentation channel from the closed spheroidal cage. The laser fluence dependence measurements indicate the first C_2 loss occurs on a microsecond time scale only at extremely high levels of excitation: more than 12.8 eV (and possibly much more). Even a "forbidden" unimolecular decay mechanism would be quite accessible at these energies.

Critical to this mechanism is the existence of a process for rapid surface geometry reorganization. Clusters like C_{60} and C_{70} (and probably all even clusters larger than C_{70}) can form spheroidal shells where no two pentagons share an edge; however, there are also other isomers of these clusters which do have this local geometry. In order to get to the adjacent pentagon transition state discussed above for C_2 loss, there must be an efficient, low energy path to moving the pentagons around on the surface of the shell. One plausible rearrangement mechanism has been suggested by Stone and Wales.[23] Like the concerted C_2 loss mechanism, this pentagon rearrangement process is forbidden by orbital symmetry considerations. Nonetheless, it may be quite facile at the high excitation energies found necessary to fragment these clusters.

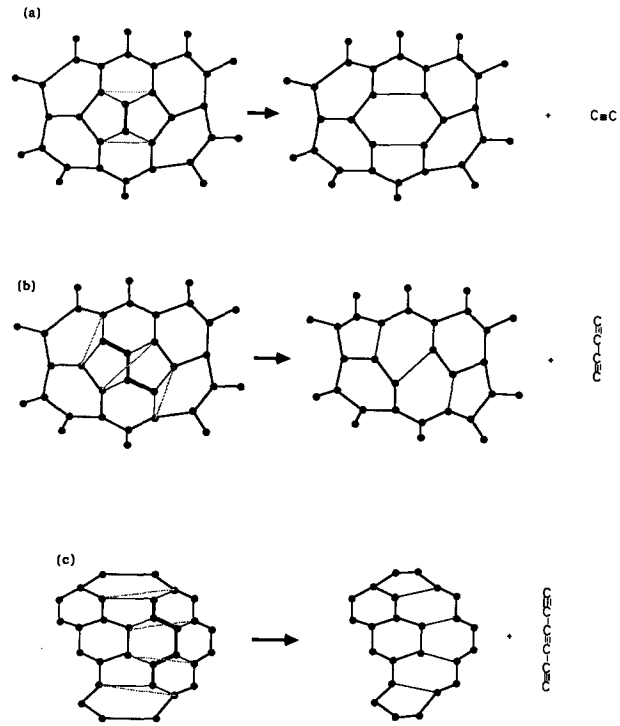

FIG. 14. Possible mechanisms for fragmentation of spheroidal carbon shells. Shown are loss of (a) C_2, (b) C_4, and (c) C_6. Loss may be in a nonsequential "unzipping" of the fragment, while the individual bond centers may undergo concerted processes.

B. Long time scale metastable fragmentation

If fragmentation were to be by sequential loss of C_2, each such loss must remove the energy binding the C_2 unit into the cage:

$$6\times 1/2\times D_{CC} - D_0(C_2),$$

where six half-bonds are broken, the C_2 bond is formed, and D_{CC} is the average carbon–carbon bond energy. In this calculation we assume the cage recloses after loss of C_2. Rough estimates of this energy give 4 eV lost per event. For C_{74}^+, 28 eV would be lost to produce C_{60}^+. While this level of excitation is reasonable, the change in unimolecular dissociation rate over a 28 eV range is enormous. One then has doubts as to whether such a sequential loss is reasonable for the very high order fragmentations. Single event C_e loss where e is an even number >2 deserves consideration as well.

The long time scale fragmentation results shown in Fig. 12 are particularly interesting and informative on this point. The interpretation of this experiment involves the creation of a highly excited species which begins to fragment immediately after excitation. Some metastable species survive the

delay to acceleration as well as the acceleration process itself, but then dissociate during the subsequent 120 μs spent in the flight tube. In these experiments there is no substantial change of the fragment patterns observed when the delay between excitation and extraction (time 1) is changed, even when the delay is as large as 15 μs. This seems incompatible with sequential C_2 loss: in the 15 μs before acceleration, any molecular system—no matter how highly excited—would have already fragmented extensively, and would no longer have sufficient energy to then fragment 7 successive times in the subsequent 120 μs, losing 4 eV per fragmentation.

Figures 14(b) and 14(c) illustrate a mechanism by which four and six carbon atoms, respectively, might be lost from a spheroidal shell with the resulting edges rejoining to form a new shell with the same number of pentagons and two and three fewer hexagons, respectively. In these losses, one can imagine the neutral carbon chain coming loose from the shell at one end with edges rejoining behind it somewhat like a zipper. We have not looked for mechanisms by which eight or more carbon atoms are lost in a single step, but guess that such mechanisms probably exist.

In the closed shell model for carbon clusters, the special numbers 70, 60, and 50 arise because these are locally good solutions to the problem of distributing the strain of closure. Photofragmentation of a closed carbon cage will require extensive excitation in order to open the cage. This will be easier for less symmetric structures where strain has concentrated at a few atoms and more difficult for symmetric, unstrained structures. The fragmentation rate will, therefore, be sensitive to the same special numbers 70, 60, and 50. Indeed, these clusters appear to be local bottlenecks in the dissociation process [see point (4) above]. The initial C_{60}^+ fragment need not be in the buckminsterfullerene structure, yet it is clear that this geometry must be sampled by the product distribution on the same time scale as fragmentation. It appears the carbon shells reclose and rapidly rearrange to the most stable structure as each C_e unit is ejected.

C_{60}^+ is a somewhat stronger fragment ion for the short time scale fragmentation process (Fig. 4) and becomes dominant in the long time scale fragmentation process (Fig. 12). The dominance of C_{60}^+ in Fig. 12 can be rationalized by the activation energy for its fragmentation being higher than that of any other cluster. In the long time scale experiments, a fragment which survives to acceleration must have a relatively low level of excitation, and for low level excitation the activation energy will have a drastic effect on the unimolecular decay rates. Thus, the most stable fragment (C_{60}^+) should have a low activation barrier to formation and be most resistant to further fragmentation, i.e., it is a bottleneck.

The large odd numbered clusters fragment to produce an even numbered shell. Note in particular in Fig. 5, that the special shell 50 is being sensed in the fragments of C_{59}^+ fragmentation. These observations suggest that the the large odd numbered clusters are also hollow shells which have closed as well as they can. Loss of an odd number of carbon atoms is followed by closure of the shell, and subsequent surface isomerization.

Perhaps, the most amazing aspect of these results is the great facility with which closure must occur. The fact that the C_e loss process breaks off so abruptly at C_{32}^+ is another indication that closure is generally achieved before further fragmentation. The result of this closure is that successively smaller closed cages are produced, a process that will ultimately end with a highly strained unstable structure.

Schmalz *et al.* have shown[20(c)] that the total strain of closure of these carbon shells is nearly a constant, independent of cluster size. As smaller and smaller closed shells are formed, the strain energy per carbon atom must increase. Independent of any other effects, at some point in this process the strain energy liberated as the transition state is formed will be sufficient to break adjacent bonds, producing even more strain release, causing the breaking of yet more bonds, etc. As a result, one expects there will be a cluster where the fragmentation process produces a complete destruction of the cage and perhaps rearrangement into rather unrelated structures. It is reasonable to expect this critical cluster will be encountered somewhere in the 30–40 atom size range since calculations show it is in this region where the open graphitic sheet structure becomes more stable.

After these experiments were completed, an independent work on fragmentation of metastable carbon clusters came to our attention.[38] These clusters were generated by laser vaporization of graphite in a vacuum, without a carrier gas and consequently are not necessarily similar in internal energies and isomer distribution. However, with few exceptions, the fragmentation patterns observed were virtually identical with those reported here.

V. SUMMARY

These photofragmentation studies can be readily interpreted in terms of these cage structures for large carbon clusters. All large even clusters appear to be closed, with the consequence that the primary photophysical fragmentation path is the loss of C_2, rather than C_3 which otherwise is the preferred fragment from a carbon cluster. The odd numbered clusters appear to be almost closed, readily losing C_1 or C_3 to become an even cluster which is closed. The smallest such spheroidal cluster formed in the beam experiments appears to be C_{32}^+. The large even clusters, and particularly C_{60}^+ are highly resistant to fragmentation, requiring very high levels of internal excitation before dissociation can occur on a microsecond time scale. If these cluster species are closed cages, then it is clear they reform and isomerize after fragmentation with amazing ease.

Although the spheroidal shell model for the large clusters of carbon is as yet unproven, it remains the only model yet advanced which is fully consistent with all known results. Its ability to explain the new, highly structured photophysical data is particularly impressive when one considers that it was originally proposed to explain only the observed abundance of the neutral clusters in a supersonic beam. Even in the absence of the original data, these new photophysics results taken by themselves would have been sufficient to force consideration of spheroidal cages in general, and the icosahedral "soccer ball" structure of C_{60} in particular.

ACKNOWLEDGMENTS

The authors would like to acknowledge extremely useful discussions with O. Cheshnovsky, H. W. Kroto, and T. G. Schmalz during our considerations of these fragmentation results. The tandem TOF apparatus used in this study is an improved version of that used previously by Brucat *et al.*[17] The improvements are largely the work of L. S. Zheng, S. Yang, C. L. Pettiette, M. J. Craycraft, and P. J. Brucat. This research was supported by the National Science Foundation and the Robert A. Welch Foundation.

[1]J. R. Heath, S. C. O'Brien, R. F. Curl, H. W. Kroto, and R. E. Smalley, Acc. Chem. Res. (in press).
[2]E. A. Rohlfing, D. M. Cox, and A. J. Kaldor, J. Chem. Phys. **81**, 3322 (1984).
[3](a) M. E. Geusic, T. J. McIlrath, M. F. Jarrold, L. A. Bloomfield, R. R. Freeman, and W. L. Brown, J. Chem. Phys. **84**, 2421 (1986); (b) M. E. Geusic, M. F. Jarrold, T. J. McIlrath, R. R. Freeman, and W. L. Brown, *ibid.* **86**, 3862 (1987).
[4]H. W. Kroto, J. R. Heath, S. C. O'Brien, R. F. Curl, and R. E. Smalley, Nature **318**, 162 (1985).
[5](a) Q. Zhang, S. C. O'Brien, J. R. Heath, Y. Liu, R. F. Curl, H. W. Kroto, and R. E. Smalley, J. Phys. Chem. **90**, 525 (1986); (b) J. R. Heath, S. C. O'Brien, Q. L. Zhang, Y. Liu, R. F. Curl, H. W. Kroto, K. F. Tittle, and R. E. Smalley, J. Am. Chem. Soc. **107**, 7779 (1985).
[6](a) Y. Liu, S. C. O'Brien, Q. Zhang, J. R. Heath, F. K. Tittle, R. F. Curl, H. W. Kroto, and R. E. Smalley, Chem. Phys. Lett. **126**, 215 (12986); (b) S. C. O'Brien, J. R. Heath, H. W. Kroto, R. F. Curl, and R. E. Smalley, *ibid.* **132**, 99 (1987).
[7]J. R. Heath, Q. L. Zhang, S. C. O'Brien, R. F. Curl, H. W. Kroto, and R. E. Smalley, J. Am. Chem. Soc. **109**, 359 (1987).
[8]S. C. O'Brien, F. D. Weiss, J. L. Elkind, R. F. Curl, and R. E. Smalley, J. Am. Chem. Soc. (submitted).
[9]M. Y. Hahn, E. C. Honea, A. J. Paguia, K. E. Schriver, A. M. Camerena, and R. L. Whetton, Chem. Phys. Lett. **126**, 251 (1986).
[10]A. O. O'Keefe, M. M. Ross, and A. P. Baronovski, Chem. Phys. Lett. **130**, 17 (1986).
[11]S. W. McElvany, H. H. Nelson, A. P. Baronovski, C. H. Watson, and J. R. Eyler, Chem. Phys. Lett. **134**, 214 (1987).
[12]A. Kaldor, D. M. Cox, D. J. Trevor, and M. Zakin, Z. Phys. D **3**, 95 (1986).
[13]D. M. Cox, D. J. Trevor, K. C. Reichmann, and A. Kaldor, J. Am. Chem. Soc. **108**, 2457 (1986).
[14]K. S. Pitzer and E. J. Clementi, J. Am. Chem. Soc. **81**, 4477 (1959).
[15]R. Hoffman, Tetrahedron **22**, 521 (1966).
[16]R. A. Davidson, Theor. Chim. Acta **58**, 193 (1981).
[17]A. D. J. Haymet, Chem. Phys. Lett. **122**, 421 (1985), J. Am. Chem. Soc. **108**, 319 (1986).
[18]R. C. Haddon, L. E. Brus, and K. Raghavachari, Chem. Phys. Lett. **125**, 459 (1986).
[19]M. D. Newton and R. E. Stanton, J. Am. Chem. Soc. **108**, 2469 (1986).
[20](a) D. J. Klein, T. G. Schmalz, G. E. Hite, and W. A. Seitz, J. Am. Chem. Soc. **108**, 1301 (1986); (b) T. G. Schmalz, W. A. Seitz, D. J. Klein, and G. E. Hite, Chem. Phys. Lett. **130**, 203 (1986); (c) T. G. Schmalz, W. A. Seitz, D. J. Klein, and G. E. Hite, J. Am. Chem. Soc. (submitted).
[21]R. L. Disch and J. M. Schulman, Chem. Phys. Lett. **125**, 465 (1986).
[22]P. W. Fowler and J. Woolrich, Chem. Phys. Lett. **127**, 78 (1986).
[23]A. J. Stone and D. J. Wales, Chem. Phys. Lett. **128**, 501 (1986).
[24]P. D. Hale, J. Am. Chem. Soc. **108**, 6087 (1986).
[25]D. S. Marynick and S. Estreicher, Chem. Phys. Lett. **132**, 383 (1986).
[26]H. P. Luthi and J. Almlof, Chem. Phys. Lett. **135**, 357 (1986).
[27]J. R. Heath, R. F. Curl, and R. E. Smalley, J. Chem. Phys. **87**, 4236 (1987).
[28]S. H. Yang, C. L. Pettiette, J. Conceicao, O. Cheshnovsky, and R. E. Smalley, Chem. Phys. Lett. **139**, 233 (1987).
[29]P. J. Brucat, L. S. Zheng, C. L. Pettiette, S. Yang, and R. E. Smalley, J. Chem. Phys. **84**, 3078 (1986).
[30]S. C. O'Brien, Y. Liu, Q. Zhang, J. R. Heath, F. K. Tittel, R. F. Curl, and R. E. Smalley, J. Chem. Phys. **84**, 4074 (1986).
[31]L. S. Zheng, P. J. Brucat, C. L. Pettiette, S. Yang, and R. E. Smalley, J. Chem. Phys. **83**, 4273 (1985).
[32]L. A. Bloomfield, M. E. Geusic, R. R. Freeman, and W. L. Brown, Chem. Phys. Lett. **121**, 33 (1985).
[33]W. C. Wiley and I. H. McLaren, Rev. Sci. Instrum. **26**, 1150 (1955).
[34]S. W. McElvany, W. R. Creasy, and A. O'Keefe, J. Chem. Phys. **85**, 632 (1986).
[35]H. W. Kroto, J. R. Heath, S. C. O'Brien, R. F. Curl, and R. E. Smalley, Astrophys. J. **314**, 352 (1987).
[36]J. R. Heath, S. C. O'Brien, R. F. Curl, H. W. Kroto, and R. E. Smalley, Comments Condensed Matter Phys. **XIII**, 3 (1987).
[37](a) K. Raghavachari, R. A. Whiteside, and J. A. Pople, J. Chem. Phys. **85**, 6623 (1986); (b) K. Raghavachari and J. S. Brinkley, *ibid.* **87**, 2191 (1987).
[38]P. P. Radi, T. L. Bunn, P. R. Kemper, M. E. Molchan, and M. T. Bowers, J. Phys. Chem. (submitted).